Tectonophysics 477 (2009) 66–76

Contents lists available at ScienceDirect

Tectonophysics

journal homepage: www.elsevier.com/locate/tecto

Mantle fault zones beneath the Himalayan collision: Flexure of the continental lithosphere

Gaspar Monsalve [a,*], Patrick McGovern [b,1], Anne Sheehan [c,2]

[a] Universidad Nacional de Colombia, Facultad de Minas, Escuela de Geociencias y Medio Ambiente, Carrera 80 No. 65-223, Medellin, Colombia
[b] Lunar and Planetary Institute, Universities Space Research Association, 3600 Bay Area Blvd., Houston, TX 77058-1113, United States
[c] University of Colorado at Boulder, Department of Geological Sciences and CIRES, UCB 399, Boulder, Colorado, 80309, United States

ARTICLE INFO

Article history:
Received 20 May 2008
Received in revised form 14 November 2008
Accepted 4 December 2008
Available online 16 December 2008

Keywords:
Himalayan collision
Focal mechanisms
Lithospheric plate flexure
Differential stresses

ABSTRACT

The Himalayas and the Tibetan Plateau are the result of the continental collision between India and Eurasia. The Indian Plate underthrusts the Himalayan mountains and the southern Tibetan Plateau. Recorded seismicity at the Himalayan collision zone suggests that earthquakes occur mainly at upper crustal depths and near the crust–mantle boundary. The question of whether the near-Moho earthquakes are in the crust or in the upper mantle has been controversial, and has raised another question about the role of the mantle in the support of mountain loads and its ability to deform by brittle processes. Earthquake locations from several experiments place seismic events in the upper mantle. Using a finite element model, we establish a link between the recorded upper mantle seismicity beneath the Himalayan collision zone and flexural bending of the Indian lithosphere. Earthquake locations, focal mechanisms, and seismic imaging results from the HIMNT experiment, combined with previous constraints on the geometry and deformation of the Himalayan collision, are used to set up the finite element models of lithospheric loading. Our purpose is to infer the mechanical state of the lithosphere beneath the Himalayas and to evaluate the role of the lithospheric mantle in the support of the loads. The pattern of mantle seismicity can be explained by modeling the response of the Indian Plate to loads corresponding to the weight of the sediments of the Ganga basin, the Himalayan mountains and the southernmost Tibetan Plateau, combined with the effects of a horizontal force per unit length acting upon the lithospheric plate. We calculated the steady-state stress field in the Indian lithosphere, where the lithospheric mantle is assumed to be viscoelastic and non-Newtonian, and the asthenosphere is modeled as viscoelastic and Newtonian. Two model suites were tested, one with an elastic crust (Model Suite 1), and one with a viscoelastic crust (Model Suite 2). Both model suites provide a good fit to the observed patterns of seismicity, but Model Suite 2 is the one that best reproduces the observations. High differential stresses concentrate in the upper mantle, and predicted principal stress orientations match those inferred from focal mechanisms in the area. Our models show that beneath the Ganga basin and the southernmost Himalaya, earthquakes at near-Moho depths do not need to show extension, nor is the lower crust required to be weak, in order to infer that the uppermost mantle yields by brittle failure. Even when flexural stresses can generate the background stresses responsible for the generation of upper mantle earthquakes, Mohr–Coulomb theory suggests that additional factors such as the presence of lateral heterogeneities or the action of pore fluids are playing a fundamental role in bringing the upper mantle materials to brittle failure.

1. Introduction

It is known that earthquakes at depths greater than 60 km below the surface occur at the Himalayan collision zone (Chen et al., 1981; Chen and Molnar, 1983; Molnar and Chen, 1983; Zhu and Helmberger, 1996; Chen and Yang, 2004). The question of whether these earthquakes are located below or above the crust–mantle boundary has been a subject of debate (Jackson, 2002; Priestley et al., 2008). Results of a recent seismic experiment in the area (Monsalve et al., 2006) suggest that brittle failure occurs at sub-Moho depths and that there is a bimodal distribution of earthquakes with depth. In this study we explore a possible cause for the generation of differential stresses that are large enough to produce these intermediate depth earthquakes in the Indian Plate.

Earthquakes occur by frictional sliding in the brittle parts of the lithosphere. When the applied stress overcomes the condition for failure, an earthquake occurs. If significant portions of the area

* Corresponding author. Tel.: +57 4 4255117; fax: +57 4 4255103.
E-mail addresses: gmonsalvem@unal.edu.co (G. Monsalve), mcgovern@lpi.usra.edu (P. McGovern), afs@cires.colorado.edu (A. Sheehan).
[1] Tel.: +1 281 486 2187; fax: +1 281 486 2162.
[2] Tel.: +1 303 492 4597; fax: +1 303 492 2606.

0040-1951/$ – see front matter © 2008 Elsevier B.V. All rights reserved.
doi:10.1016/j.tecto.2008.12.014

encompassed by the yield strength envelope of the lithosphere include sub-Moho depths, then the upper mantle participates in the support of the loads acting on the lithospheric plate. An indication that the lithospheric mantle just south of the Himalayan collision participates in the support of the loads applied to the Indian Plate has been given by recently obtained values of elastic thickness (Jordan and Watts, 2005; Hetényi et al., 2006), which represent a measure of the integrated strength of the lithosphere (Watts, 2001; Watts and Burov, 2003; Burov and Watts, 2006). These values indicate that at least in some areas of the India–Eurasia collision zone, the elastic thickness is greater than the crustal thickness. For instance, Jordan and Watts (2005) found that in the foreland of the Central Himalaya the elastic thickness is about 70 km, whereas Moho depths in this region are below 50 km (Mitra et al., 2005). Given those conditions, if stresses in the uppermost mantle are high enough to reach the failure envelope, subcrustal earthquakes take place.

It is widely accepted that most of the seismicity in the continental lithosphere is confined to its crustal portion (Maggi et al., 2000a,b; Jackson, 2002; Mouthereau and Petit, 2003; Burov and Watts, 2006; Priestley et al., 2008) and earthquakes in the upper mantle are rare. However, the presence or absence of earthquakes is not by itself an indicator of the amount of stress borne by a material layer (Watts and Burov, 2003); seismicity merely requires the brittle strength of a layer be exceeded. Since brittle strength increases with pressure, we might expect the high lithostatic pressures at mantle depths beneath the Himalaya are consistent with a relative absence of seismicity. Thus, the upper mantle can be considered to be strong if it bears a significant fraction of the stresses required to support observed loads, regardless of the presence or absence of seismicity. Nonetheless, seismicity indicates the locations where locally high stresses, perhaps aided by mitigating factors like pore fluid pressure, approach a yield condition.

Earthquakes beneath the Himalayan collision zone occur due to a variety of causes. The India–Eurasia convergence, where the top of the Indian Plate slides beneath the Himalaya and Southern Tibet, generates compressional strain that accumulates in the Himalaya, which is responsible for the great Himalayan Earthquakes (Cattin and Avouac, 2000; Bilham et al., 2001; Bilham, 2004; Feldl and Bilham, 2006). In contrast, upper-crustal earthquakes in southern Tibet, at depths shallower than the top of the underthrusting Indian Plate, indicate east–west extension (de la Torre et al., 2007), possibly driven by gravitational collapse of the southern Tibetan Plateau (Molnar and Tapponnier, 1978). The lithospheric plates respond to loading by flexing and yielding (Watts, 2001) and, as stated by Burov and Diament (1995), the bending stresses that mountain belts create are large enough to generate brittle failure. For the case of the Himalayan collision, the bending stresses in the Indian plate can be included as a potential cause for earthquakes within it. This kind of stresses has been invoked as a cause for intraplate earthquakes in India, south of the Himalayan front (Bilham et al., 2003; Bilham, 2004). Crustal and upper mantle earthquakes in the oceanic lithosphere have also been explained by flexural bending of the lithospheric plate beneath volcanic islands (Thurber and Gripp, 1988; Wolfe et al., 2003; Pritchard et al., 2007; McGovern, 2007). In the next sections, we explore and discuss the plausibility of the flexure of a layered lithosphere beneath a mountain load to produce stress magnitudes and orientations at locations consistent with the observed seismicity.

2. Event location and upper mantle earthquakes

Most of the crustal earthquakes in the Himalayan collision zone occur in the thrust sheets overlying the Indian Plate, above the Main Himalayan Thrust (Pandey et al., 1995; Monsalve et al., 2006). However, two clusters of earthquakes are located at near-Moho depths beneath the Sub/Lesser Himalaya and the Greater/Tethyan Himalaya. (Monsalve et al., 2006) provided evidence that at least one earthquake in each cluster occurred below the Moho. We have performed additional relocation of local earthquakes recorded by the

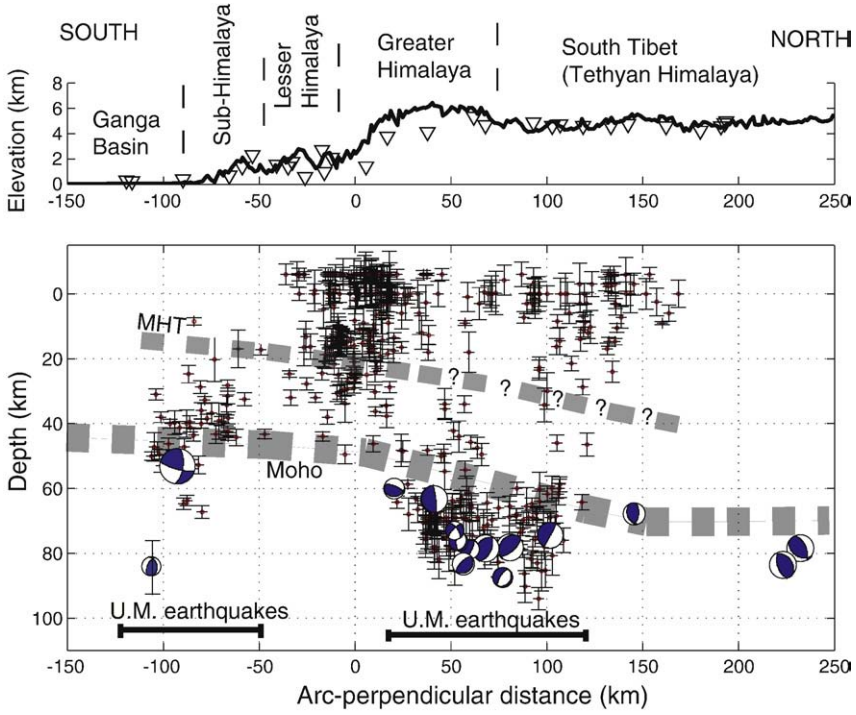

Fig. 1. Relocation of HIMNT local seismic events (earthquakes with ten or more associated arrivals) projected onto a Himalayan-arc perpendicular cross-section (distances are relative to an approximate location of the Himalayan arc), using a probabilistic non-linear locator and the final 2-D model from Monsalve et al. (2008). Error bars indicate one standard deviation uncertainties. Gray dashed lines correspond to the Moho and the Main Himalayan Thrust (MHT, which is interpreted as the top of the Indian Plate) from Schulte-Pelkum et al. (2005); their thicknesses indicate the mean uncertainty. Question marks are associated to places where the MHT is not clearly defined. Triangles denote projections of HIMNT station locations onto the cross-section. Horizontal black bars labeled as 'U.M. earthquakes' represent the range of arc-perpendicular distances at which earthquakes were located in the upper mantle by Monsalve et al. (2006). Western hemisphere focal mechanisms for earthquakes in the area around Moho-depths are also shown (de la Torre et al., 2007).

Table 1
Density (ρ), elastic parameters (Young's modulus E and Poisson's ratio ν), cohesion C, and internal friction angle ϕ for the crust and the mantle lithosphere used for model suites 1 and 2.

Parameter	Crust	Mantle lithosphere
ρ(kg m^{-3})	2750	3270
E(Gpa)	30	80
ν	0.25	0.25
C(MPa)	10	10
ϕ	30°	30°

HIMNT network with ten or more associated arrivals; Fig. 1 shows these event locations projected onto a Himalayan arc-perpendicular cross-section. For the relocation work, we use a two-dimensional velocity model obtained from joint-inversion for earthquake location and velocity structure (Monsalve et al., 2008), with a probabilistic non-linear location algorithm ((Lomax, 2004, Fig. 1).

A cluster that includes upper-mantle earthquakes is located in South Nepal, at arc perpendicular distances between −120 and −50 km (Fig. 1), roughly at the latitude of the Main Frontal Thrust fault outcrop. Most of these events are likely related to the1988 Udaypur earthquake. Unfortunately, none of the events from this cluster recorded by the HIMNT (Himalayan Nepal Tibet seismic experiment) network (Monsalve et al., 2006) had high enough quality associated seismograms to run a whole moment tensor waveform inversion (de la Torre et al., 2007). The m_b 6.5, 08-20-1988 Udaypur earthquake, was assigned a depth of 51 ± 5 km (Chen and Kao, 1996), which is an upper mantle depth at this location, and the focal mechanism indicates north–south thrust faulting (Fig. 1). Around 200 km to the west of this cluster, there was an upper mantle earthquake recorded by the HIMNT network; its depth was determined to be 84 km and its focal mechanism indicates strike-slip faulting with a near Himalayan arc-perpendicular P-axis (de la Torre et al., 2007, Fig. 1).

Another group of uppermost-mantle earthquakes is located beneath the Greater Himalaya and Southern Tibet, at arc-perpendicular distances between 20 and 120 km (Fig. 1). de la Torre et al. (2007) determined focal mechanisms for 8 earthquakes in this area recorded by the HIMNT network, and integrated them with previously published focal mechanisms for intermediate depth earthquakes in the region (Chen et al., 1981; Molnar and Chen, 1983; Zhu and Helmberger, 1996; Engdahl et al., 1998). The focal mechanisms for these earthquakes at near-Moho depths suggest a predominantly strike-slip type of faulting, with near horizontal P-axis in a N–S direction (nearly arc-perpendicular) and shallow plunging T-axis in an E–W direction (approximately arc-parallel) (Fig. 1).

3. Flexural modeling

In order to elucidate the possible role of flexural bending of the Indian Plate in the upper-mantle seismicity, we use a finite element method to calculate the stress field in the lithosphere after viscoelastic relaxation of the mantle. This allows us to determine the magnitude and orientation of the principal stresses in the lithosphere. We assume elastic and visco-elastic regimes in a vertically layered lithosphere, and that materials behave as a Maxwell's solid. The finite element code TEKTON (Melosh and Raefsky, 1980, 1983) was used to model the displacements and stresses that result from the lithospheric bending of the Indian Plate due to the weight of the mountains and thrust sheets above the Main Himalayan Thrust fault, and the horizontal compression resulting from the plate convergence. We assume plane strain and cartesian coordinates on a representative vertical cross-section of the Indian Plate at the location of the continental collision. The stresses and displacements that the finite element code calculates appear in response to a load-induced viscoelastic regime in the lithosphere and the asthenosphere. We let the system evolve for a long enough time T so that the subsidence of the plate stops and the system reaches a steady state. For our models, $T = 5500T_M$, where $T_M = (2(1+\nu)\eta)/E$, is the asthenospheric mantle relaxation time, ν is the Poisson's ratio, η is the viscosity and E is the Young's modulus.

Once the final differential stress is calculated for each element, the proximity to failure is evaluated using the Mohr–Coulomb criterion, which relates shear stress at failure τ to normal stress σ_n,

$$\tau = C + \sigma_n \tan\phi, \quad (1)$$

where C is the cohesion of the materials and ϕ is the internal friction angle. The values we used for these parameters are shown in Table 1.

The finite element models that we present are simplifications of processes that operate at the Himalayan collision. They do not intend to replicate the exact pattern of observed seismicity, nor to reproduce the exact physical conditions of the Indian lithosphere in the collision zone, but to evaluate plausible causes for the occurrence of earthquakes in the

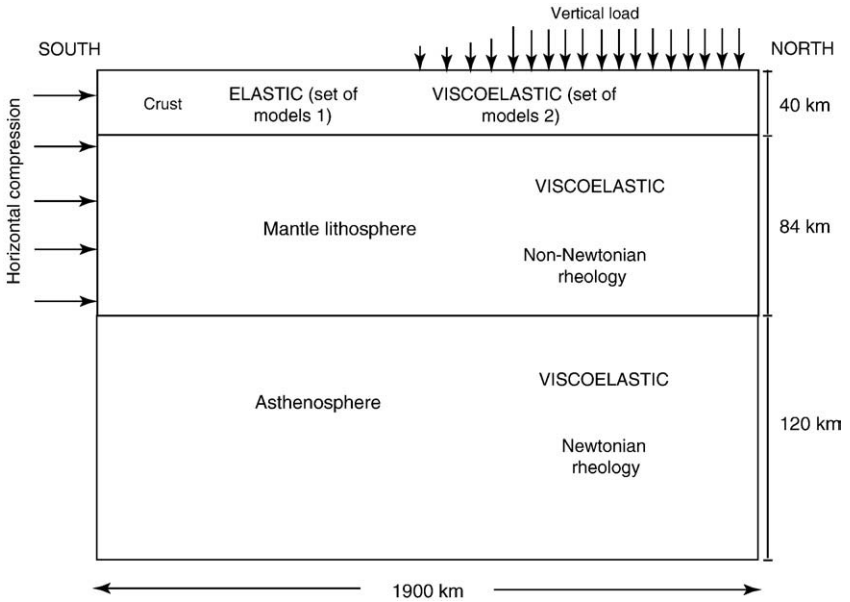

Fig. 2. Geometry of the lithosphere–asthenosphere system that we use for the finite element modelling. Arrows on top of the lithosphere represent the vertical load (sediments, mountains and rocks overlying the Indian Plate). Horizontal compression is denoted by arrows on the left.

Indian Plate beneath the Himalayas. For this reason, we limit our analysis to the Indian Plate and we do not calculate stresses within the materials on top of it.

3.1. Material properties, rheology, geometry and boundary conditions

For all of our models, the asthenosphere is assumed to be isoviscous and Newtonian, with a viscosity of 10^{20} Pa s, consistent with recent findings by Mitrovica and Forte (2004), Steinberger and Calderwood (2006), and Paulson et al. (2007); the Young's modulus is assumed to be 100 GPa, and the Poisson's ratio and density are 0.25 and 3300 kg m^3 respectively. These values of viscosity, Poisson's ratio and Young's modulus give a relaxation time for the asthenospheric mantle T_M of approximately 80 years. For the rheological layering of the lithosphere, we considered two situations: (1) A homogeneous elastic crust and a viscoelastic lithospheric mantle with viscosities given by Molnar and Jones (2004), and (2), a layered viscoelastic crust overlying a viscoelastic mantle with viscosities given by a power law rheology (Goetze, 1978). We explore those two model suites, so that we can evaluate the role of the mantle in the support of the loads under different assumptions about the strength of the crust. A description of each Model Suite is given below.

Fig. 2 shows the basic geometry that we use for our numerical experiments. For the models we show below, we worked with square elements of 8 km by 8 km. Displacement boundary conditions are defined such that nodes on the north edge of the model are fixed in the horizontal direction but free in the vertical, nodes at the bottom of the model are free in the horizontal direction and fixed in the vertical, and corners at the bottom are fixed in both directions. Nodes at the top of the plate have free displacement in the horizontal direction (except at the corners) and experience constant force in the vertical direction (the weight of the load).

Since we are studying a region of continental collision where the Indian Plate bends under the action of loads applied on it, we should explore not only the effects of the weight of the sediments in the Ganga basin and the overthrust sheets and mountains, but also the action of a horizontal force per unit length: given that the Indian Plate is underthrusting the Himalayas and Southern Tibet, it is necessary to consider the in-plane compression that appears from mantle drag forces and from shear forces exerted by the material above the Indian Plate. This in-plane compression is invoked by Mueller and Phillips (1995) when considering stresses from drag on subducting plates. For simplicity, we assume that such a compression is horizontal, and we simulate it by imposing a progressive northward displacement of the far south boundary of the model (Fig. 2). The vertical load on top of the Indian Plate is modeled using a representative cross-section of a Himalayan arc-perpendicular topography and the approximate location of the top of the Indian Plate (the Main Himalayan Thrust) projected onto an arc-perpendicular direction (from Zhao et al., (1993), Schulte-Pelkum et al., (2005), and Hetényi et al., (2006)). The load includes the sediments of the Ganga basin as well as the Himalayan mountains and the southern Tibetan Plateau. We made the load slightly less dense than the crustal portion of the Indian lithosphere.

One of the main factors that controls viscous flow in the lithosphere is the temperature. We do not intend to incorporate the whole time evolution of the temperature field in the region of the Himalayan collision, but to use reasonable vertical geothermal gradients that can represent known constraints on the thermal structure of the Indian Plate in this area. We work with an approximation of a model proposed by Henry et al. (1997), which they found to reproduce many of the known metamorphic conditions in the crust. It is associated with a mantle heat flow of 15 mW/m^2 and an upper crust heat production of 2.5 μW/m^3. For our calculations, we assume that the temperature profile across the Indian lithosphere that underthrusts the Himalayas and southern Tibet goes from 473 K at the top of the plate to 1073 K at the base, with Moho temperatures varying from 600 to 900 K.

3.1.1. Model Suite 1

We defined an elastic crust and a viscoelastic non-Newtonian lithospheric mantle. By making these assumptions we intend to explore the possibility of the upper mantle supporting large differential stresses even in those cases where there is no ductility in the lower crust. For the elastic crust, we worked with a set of plausible parameters (E and ν) for compositions predominantly consisting of quartz and diabase, utilizing values similar to those used by Cattin and Avouac (2000) and Hetényi et al. (2006). In Table 1 we show the set of parameters that we assumed for all cases.

For the viscoelastic upper mantle, we used the formulation of Molnar and Jones (2004), who derived expressions for temperature-dependent viscosity coefficients for olivine and eclogite, appropriate for high differential stress and low temperature creep laws proposed by Goetze (1978) and Goetze and Evans (1979). Molnar and Jones (2004) calculated an effective viscosity using a weighted average of viscosities calculated by a power law relationship and the Dorn law (Goetze, 1978). For a non-Newtonian flow, the relation between deviatoric stress, τ_{ij}, and strain rate, ε_{ij}, is given by (as in Molnar and Jones (2004)):

$$\tau_{ij} = BE^{(1-n)/n}\varepsilon_{ij}, \tag{2}$$

where B is the viscosity coefficient, and E^2 is the second invariant of the strain rate tensor. When the differential stress is less than 200 MPa (Goetze, 1978), B is a function of temperature (T):

$$B_{\text{LowStress}}(T) = \frac{1}{\sqrt[n]{2A}}\exp\left(\frac{H_a}{nRT}\right), \tag{3}$$

A is the power law strain rate, n is the power law exponent, H_a is the activation enthalpy, and R is the universal gas constant. At higher stresses and temperatures less than 1000 K, B is a function of T and E (Molnar and Jones, 2004):

$$B_{\text{HighStress}}(T,E) = \frac{\sigma_0}{E\sqrt{3}}\left[1-\left(\frac{RT}{H_a}ln\frac{\sqrt{3}\varepsilon_0}{2E}\right)^{\frac{1}{2}}\right]. \tag{4}$$

In this equation, $\sigma_0 = 8.5$ GPa and $\varepsilon_0 = 5.7*10^{11}$ s^{-1} are experimentally determined constants for dry olivine (Goetze, 1978). By weighting $B_{\text{LowStress}}$ and $B_{\text{HighStress}}$, Molnar and Jones (2004) obtain an expression for the effective value of B:

$$\frac{1}{B_{\text{effective}}(T,E)} = \frac{1}{B_{\text{LowStress}}(T)} + \frac{1}{B_{\text{HighStress}}(T,E)}. \tag{5}$$

We used parameters for 'dry' olivine, with a power law exponent $n = 3.5$, activation enthalpy $H_a = 540$ KJ mol^{-1}, and power law strain rate $A = 2.4*10^5$ MPa^{-n} s^{-1}. For a more complete description and justification of the use of these laws for uppermost mantle rocks see Molnar and Jones (2004).

3.1.2. Model Suite 2

In contrast with the previous Model Suite, in the second Model Suite a viscoelastic crust is divided in two layers, with an interface at a depth of 16 km below the top of the Indian Plate, and we use a power law relationship (Eq. (3)) to calculate the effective viscosity in the lithosphere. The main purpose of using this suite of models is to evaluate the role of the lithospheric upper mantle in the support of the loads when some ductility is allowed in the crust; at the same time, we can visualize the effects of the use of a power law rheology in the mantle, which is an extrapolation from differential stresses lower than those at the upper lithospheric mantle beneath the Himalayas

Table 2
Rheological parameters for the Indian lithosphere used for Model Suite 2.

Parameter	Dry quartzite (upper crust)	Diabase (lower crust)	Wet dunite (upper mantle)
$A(\mathrm{MPa}^{-n}\,s^{-1})$	1.585×10^{-7}	6.31×10^{2}	398
n	2.9	3.05	4.5
$H_a(\mathrm{kJ\ mol}^{-1})$	149	276	498

Taken and modified from Cattin and Avouac (2000) and Hetényi et al. (2006); A, Power law strain rate; n, power law exponent; H_a, power law activation energy.

(Goetze, 1978). The upper crust is assumed to be composed by dry quartzite, the lower crust by diabase and the lithospheric mantle by wet dunite (Cattin and Avouac, 2000; Hetényi et al., 2006). For the elastic parameters, we use values from Table 1. Table 2 shows the chosen parameters for the power law creep equation when using this Model Suite.

3.2. Results

The TEKTON finite element code calculates horizontal and vertical normal stresses and in-plane shear stresses at every element, which we transform into principal stress axes. The conventions for the orientation of the principal stresses σ_1 and σ_3, where σ_1 is the most compressive principal stress and σ_3 is the least compressive one, follow McGovern and Solomon (1993, 1998), and the symbols are illustrated in Fig. 3. An approximation to the principal stress orientation and predicted type of faulting that we should expect to obtain according to the upper mantle earthquake locations in the area, the focal mechanisms in Fig. 1, and the average results of the P and T axes for earthquakes deeper than 60 km in de la Torre et al. (2007), is shown in Fig. 4. A result of the finite element model applied to the Indian Plate at the Himalayan collision, for the case of an elastic crust (Model Suite 1) can be seen in Fig. 5.

The ranges of arc-perpendicular distances at which clusters of near-Moho earthquakes occur, roughly located south of the front of the Himalaya and beneath the transition from the Greater Himalaya to southern Tibet (black horizontal bars in Figs. 1, 4 and 5), coincide with regions of high curvature of the flexed plate and opposite concavity. South of the topographic front of the Himalaya (negative coordinates along the X-axis in Fig. 5), the flexure is concave-down and there is arc-perpendicular extension at the top, which evolves to nearly arc-perpendicular compression at greater depths. In southern Tibet, at locations with positive coordinates along the horizontal axis, the flexure is concave-up, and the state of stresses is highly determined by whether or not we include horizontal compression in our models.

Fig. 5 illustrates the stress field for two cases, which represent two different boundary conditions. For the case of no horizontal compression (Fig. 5a), we see that in the Himalayan foreland both the crust and the uppermost mantle are under near-horizontal arc-perpendicular extension, switching to near-horizontal arc-perpendicular compression at depths greater than 60 km. This reflects a bias toward extension produced by the overall lengthening of the initially flat lithosphere by bending, and it is a consequence of ignoring the in-plane horizontal forces acting on the plate. According to what is known about the variation of focal mechanisms with depth in the Himalayan foreland (Jackson, 2002), this transition from normal to thrust faulting should occur in the lower crust and not in the mantle. The addition of horizontal compression allows a better fit to the observations (Fig. 5b), so that such a switch in stress orientations beneath the Ganga basin and the southernmost Himalaya takes place in the lower crust, and the predominant stress orientations at this location are consistent with the known focal mechanisms of earthquakes in the area. For instance, the focal mechanism of the 1988 Udaypur earthquake, which is most likely located in the upper mantle (Chen and Kao, 1996), indicates near-horizontal arc-perpendicular thrust faulting, consistent with what is predicted by the model.

Principal stress orientations in the uppermost mantle beneath southern Tibet are consistent with strike-slip faulting when horizontal compression is absent (Fig. 5a), roughly coinciding with what is observed from focal mechanisms in the area (Fig. 1).The addition of compression causes the vertical stress in the uppermost mantle to be of a magnitude similar to that of the out-of-plane principal stress, so that in some cases the stress orientations are consistent with thrust faulting. An example of this situation can be seen in Fig. 5b: beneath the transition from the Greater Himalaya to southern Tibet, where a cluster of upper mantle earthquakes is located, the stress orientations predict strike-slip faulting in the uppermost mantle, matching observations from focal mechanisms, whereas to the north there is a transition to a stress regime consistent with thrust faulting.

Fig. 6 shows vertical variations of stress differences and proximity to failure, for the case of an elastic crust (Model Suite 1), at the average location of the two clusters of HIMNT earthquakes at upper mantle depths (black horizontal bars in Figs. 1, 4 and 5), for different amounts of horizontal compression. Fig. 6a and b shows the difference between in-plane stresses, so that we can identify regions of compression (negative stress differences) and extension (positive stress differences) on a Himalayan arc-perpendicular cross-section of the Indian plate. Similarly, Fig. 6c and d shows proximity to failure, calculated using Eq. (1). According to what is known about the variation with depth of focal mechanisms of earthquakes beneath the Gangabasin (Jackson, 2002), values of horizontal compression equivalent to displacements of the southern end of our finite element grid of 22 and 32 km (black and red curves in Fig. 6) are the ones that best fit the observations, with the depth of the neutral surface (depth at which stress differences are zero) at the lower crust of the Indian Plate. The inclusion of this horizontal force in our model causes most of the Indian lithosphere in the Himalayan collision zone to be in a compressional regime, different from what is predicted when it is only under the effect of the weight of rocks above the Main Himalayan Thrust, where most of the lithosphere at the locations of the upper mantle earthquakes is in extension (green curves, Fig. 6a and b). For the case of the Greater Himalaya and the southernmost Tibetan plateau, the whole lithosphere could be under compression (black and red curves, Fig. 6b). In general, the highest values of proximity to failure take place in the upper crust (Fig. 6c and d), and as horizontal compression is added to the model, a local maximum appears in the uppermost mantle (blue, black and red curves, Fig. 6c and d).

When the crust is assumed to be viscoelastic and a power law relationship is used for the whole lithosphere (Model Suite 2, Fig. 7), horizontal compression causes the differential stress orientations to

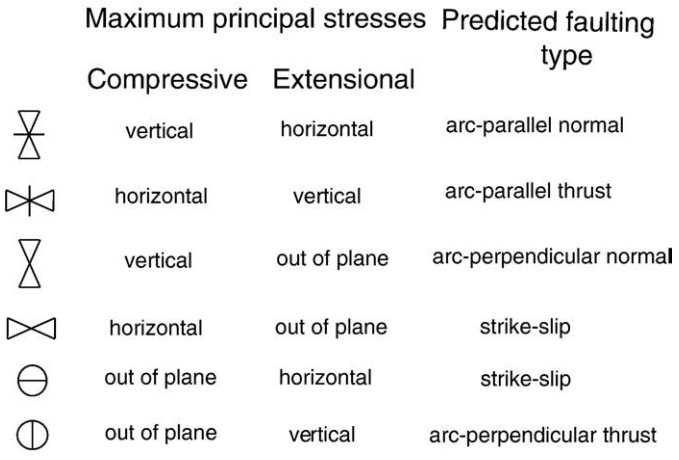

Fig. 3. Stress symbols for the case of horizontal and vertical principal stresses. The hourglass shapes are oriented along the direction of maximum compressional stress (σ_1) and the bars are oriented along the direction of maximum extensional stress (or minimum compressional σ_3) (modified from McGovern and Solomon (1993, 1998)).

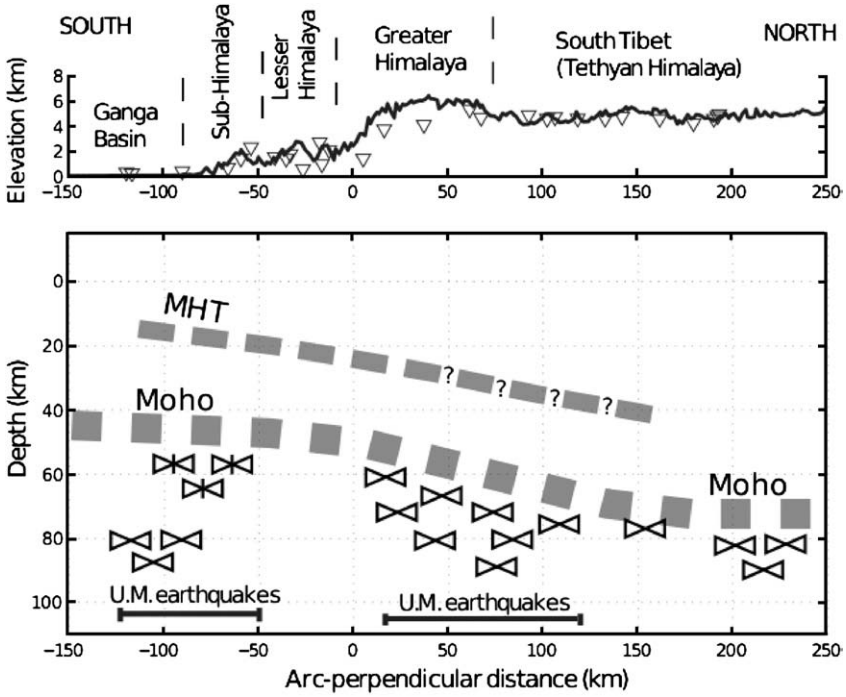

Fig. 4. Schematic Himalayan arc-normal view of approximate principal stress orientations associated with the focal mechanisms from Fig. 1. The horizontal bars at the bottom of the models (labeled as 'U.M. earthquakes') represent the location of clusters of earthquakes at near-Moho depths from the HIMNT experiment (Monsalve et al., 2006). We are assuming that two of the principal stresses are contained in the arc-normal plane, which is a good approximation according to results from de la Torre et al. (2007). See Fig. 3 for symbol conventions.

be similar to those obtained using Model Suite 1 (Fig. 5b). However, the overall results from Model Suite 2 give the best match to the observations (Figs. 4 and 7). There are two important variations in Model Suite 2 relative to Model Suite 1: stress orientations in the uppermost mantle beneath the transition from the Ganga basin to the Sub-Himalaya are consistent with strike-slip faulting and not with thrusting. In this case, as it was mentioned above, the magnitude of the out-of-plane principal stress is similar to that of the vertical stress. The presence of inhomogeneities, previous faulting or pore pressures could easily switch the type of faulting at this location. The second variation is the absence of stress orientations consistent with thrust faulting in the uppermost mantle beneath the Greater Himalaya and Southern Tibet (Model Suite 2, Fig. 7); stress orientations exclusively suggest strike-slip faulting, as most of the focal mechanisms at these depths indicate. In terms of the magnitude of the stress, Fig. 7 shows that differential stresses greater than 800 MPa occur only in the mantle portion of the lithosphere, different from the model in Fig. 5b, where the highest differential stresses occur in the upper Indian crust beneath Southern Tibet. The highest differential stresses take place in the uppermost mantle beneath Southern Tibet. There is also a region of high differential stresses (greater than 1 GPa) beneath the Ganga basin, at depths between about 70 and 90 km (more than 30 km below the Moho), and there is no significant contrast in the magnitude of the differential stress (less than 200 MPa) between the lowermost crust and the uppermost mantle at this location.

Fig. 8 is analogous to Fig. 6, and it illustrates the effects of horizontal compression in the case of a layered viscoelastic crust (Model Suite 2). Since the non-elastic effects prevail at the lowermost crust, we did not extrapolate the curves in the lower crust all the way to the Moho, and did not connect their crust and mantle segments. The effects of the addition of horizontal compression are similar to those illustrated in Fig. 6 (for the case of the elastic crust) in that most of the lithosphere is under compression. For the cases of horizontal compression equivalent to a displacement of the southern end of the finite element grid of 17 and 22 km (black and red curves respectively), we see that the neutral surface beneath the transition from the Ganga basin to the Sub-Himalaya (Fig. 8a) is in the lower Indian crust, consistent with the focal mechanism data (Jackson, 2002). In contrast with the cases plotted in Fig. 6a, where the greatest stress differences occur near the top of the mantle, curves in Fig. 8a show that the greatest stress differences take place at more than 40 km below the Moho. Overall, Figs. 8b and 6b show a similar pattern, but the offset in stress difference across the Moho is greater for the case of a viscoelastic crust (Fig. 8b). As expected from the magnitude of differential stresses at the locations of the upper mantle earthquakes (Fig. 7), when horizontal compression is included in the model, the values of proximity to failure in the lithospheric mantle are maximum at depths greater than 80 km beneath the transition from the Ganga basin to the Sub-Himalaya (Fig. 8c) and at uppermost mantle depths beneath the Greater Himalaya and Southern Tibet (Fig. 8d).

4. Discussion

The seismicity recorded by the HIMNT network reveals the existence of earthquakes in the upper mantle at two main locations along a Himalayan arc-perpendicular cross-section: the transition from the Ganga basin to the Sub-Himalaya, and the transition from the Greater Himalaya to southern Tibet (Fig. 1), in places of high curvature of the flexed Indian Plate. The finite element models show regions of high differential stresses in the uppermost mantle, with orientations that match those inferred from focal mechanisms of earthquakes in the area.

In support of the idea that all earthquakes in this region are above the Moho, Jackson (2002) argues that if the deep earthquakes beneath the southernmost Himalaya and the foreland were in the upper mantle, they would show extension and not thrusting (as the observations show and our models predict). The magnitude and orientation of stresses in Fig. 5a beneath the Ganga basin and the green curve of Fig. 6a suggest an approximation to the kind of situation that Jackson (2002) would expect to support the idea of earthquakes in the upper mantle: stresses in the uppermost crust and uppermost mantle are consistent with arc-normal extension,

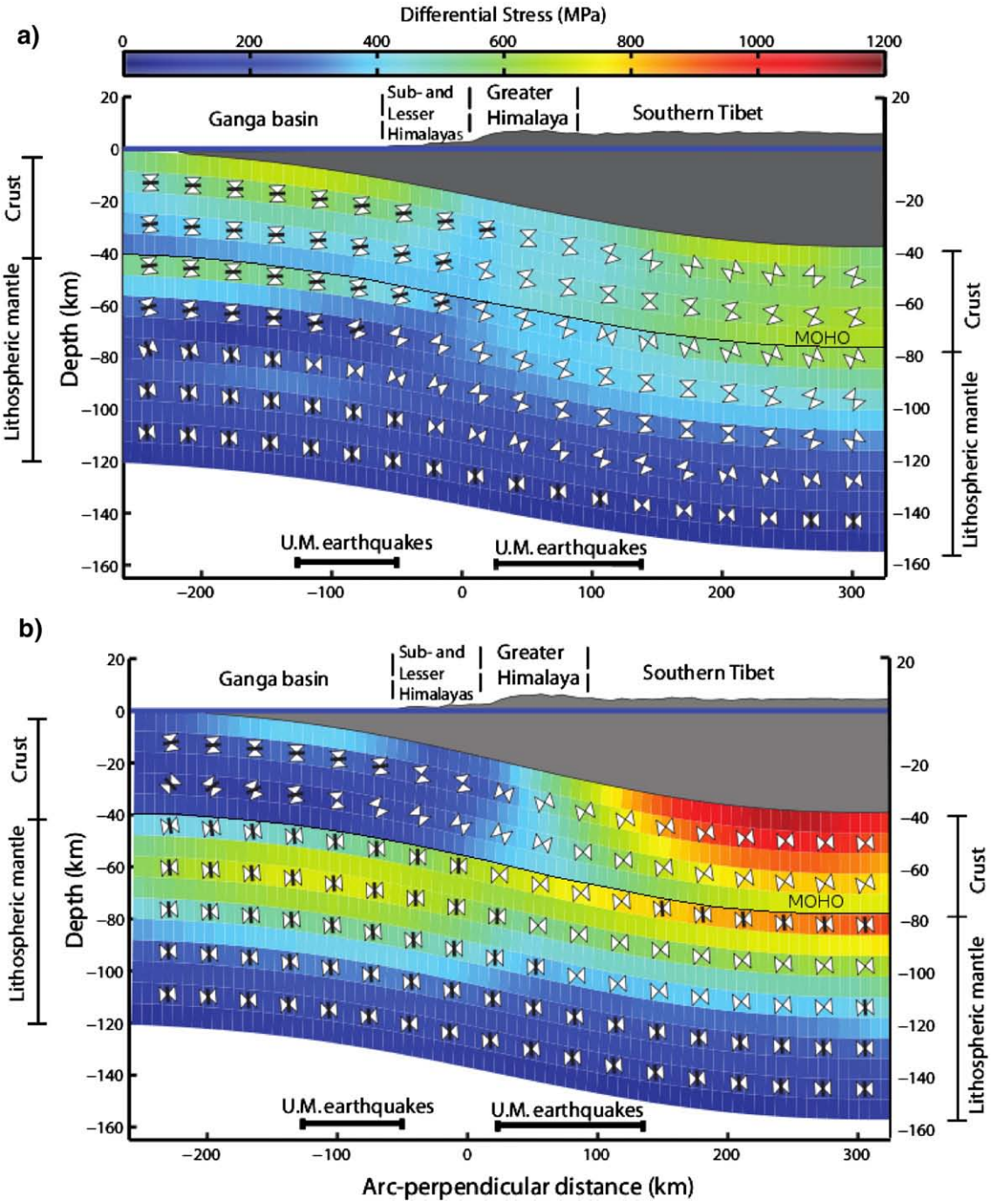

Fig. 5. Flexural profile and stress field along a Himalayan arc-perpendicular cross-section across the study region for an elastic crust (Model Suite 1). Two cases are illustrated: a) No horizontal compression, and b) inward displacement of the southern edge of the model of 22 km. The horizontal bars at the bottom of the models (labeled as 'U.M. earthquakes') represent the location of clusters of earthquakes at near-Moho depths. See Fig. 3 for symbol conventions.

predicting normal faulting. In the same manner, the green curve in Fig. 8a shows extension in the upper crust and the uppermost mantle. However, addition of horizontal compression suppresses this kind of behavior: the crust is under extension in its upper part, becomes less extensional at greater depths, and for some cases, its lowest part is under compression (i.e. black and red curves from Figs. 6a and 8a); in the uppermost mantle, instead of switching back to extension (or a less compressional state), the horizontal stress becomes even more compressional. In those models where viscoelasticity is allowed in the crust (Figs. 7 and 8), stresses in the uppermost mantle do not predict extension when horizontal compression is taken into account. There are some cases, for the two suites of tested models, in which the lithosphere works almost as a continuum, with no significant jumps in stress difference across the Moho (blue curve in Fig. 6a and black curve in Fig. 8a). Thus, these models suggest that earthquakes in the uppermost mantle beneath the Ganga Basin and the southernmost Himalaya can show thrusting, and not necessarily extension. According to these observations, Jackson's argument cannot be used as a piece of evidence that all the earthquakes in the area should occur above the Moho.

Comparison of Fig. 5a and b beneath the Greater Himalaya and Southern Tibet suggests that the addition of horizontal compression enhances the contrast in magnitude of differential stresses between the lowermost crust and the uppermost mantle. The green curve from

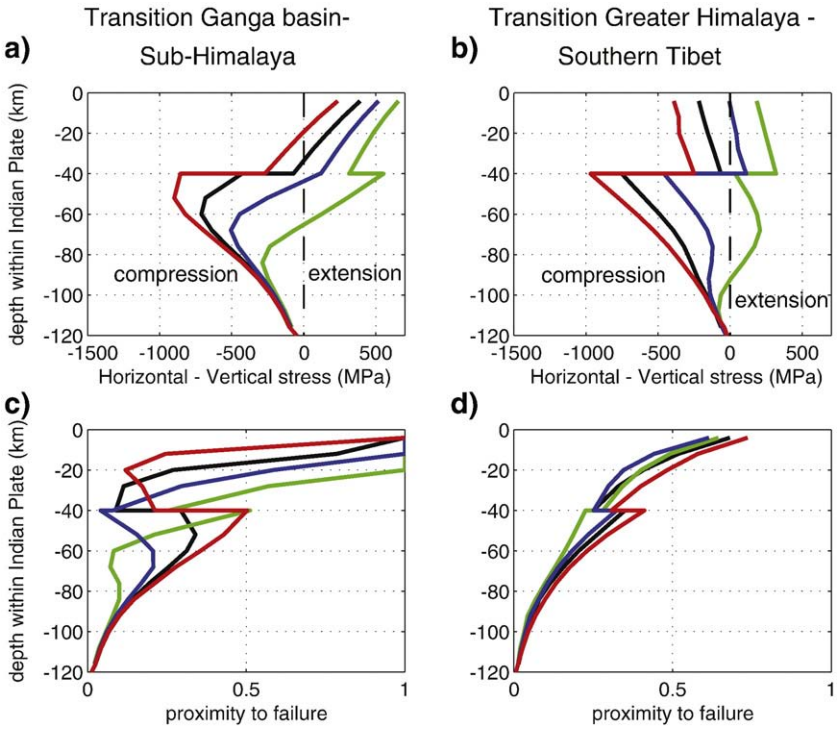

Fig. 6. Cross-sections of stress differences at the average locations of clusters with upper mantle earthquakes for different amounts of horizontal compression. Results from Model Suite 1 are shown here. Green curves represent the case of no horizontal compression; blue, black and red curves represent displacements of the southern end of the model of 12, 22, and 32 km respectively. a) Stress differences at the transition Ganga Basin–Sub-Himalaya, b) stress differences at the transition Greater Himalaya– Southern Tibet, c) proximity to failure at the transition Ganga Basin–Sub-Himalaya, d) proximity to failure at the transition Greater Himalaya–Southern Tibet.

Fig. 6b shows an offset across the Moho towards a more compressional state of stress in the uppermost mantle; the addition of horizontal compression enhances this offset (blue, black and red curves). Something similar can be seen in Fig. 8b. This contrast of differential stresses across the crust–mantle boundary (for all the cases that account for horizontal compression) is consistent with the fact that deep earthquakes at this location predominantly cluster below the Moho (Fig. 1). Also, for the models with horizontal compression, proximity to failure at this location is greater in the uppermost mantle than in the lowermost crust.

Even though there is not a single model that replicates exactly the pattern of seismicity in Figs. 1 and 4, the different models presented are consistent with focal mechanisms of earthquakes at around Moho depths and below. Earthquakes at around Moho depths beneath the transition from the Greater Himalaya to Southern Tibet predominantly show strike-slip faulting with a nearly arc-perpendicular compressional axis. Stress orientations in the uppermost mantle beneath this location, predicted by models in Figs. 5b and 7, coincide with those focal mechanisms. There are some near-Moho earthquakes in south Tibet to the north of this cluster (Molnar and Chen, 1983; Zhu and Helmberger, 1996), shown in Fig. 1 at arc-perpendicular distances between 200 and 250 km, where the predominant focal mechanisms are strike-slip with *P*]axis approximately arc-perpendicular (see Fig. 4): the model in Fig. 7 matches those focal mechanisms; the model in Fig. 5b suggests thrust faulting at this location, but the magnitude of the out-of-plane principal stress is similar to that of the vertical stress, so that when earthquakes are triggered, either one of these principal stresses could be enhanced and any of these two types of faulting could occur.

Unfortunately, for the area of the HIMNT experiment, there are not many available earthquakes beneath the Sub-Himalaya and the Ganga basin with focal mechanisms that can be used to compare with our models. The 1988 Udaypur earthquake, at a depth of 51 km (Chen and Kao, 1996) (arc-perpendicular distance of around −90 km in Fig. 1), indicates thrust-faulting consistent with arc-perpendicular compression (Fig. 4). The model in Fig. 5b reproduces the thrust faulting in the uppermost mantle, consistent with the focal mechanism of this earthquake. The model presented in Fig. 7, where effective viscosities are calculated using power law rheologies, indicates some strike-slip faulting in the upper mantle beneath the Ganga basin. For the case of the uppermost mantle, at the location of the Udaypur earthquake, the difference between the vertical and the out-of-plane stresses is below 50 MPa, so that changes in the magnitude of the sediment load, the effects of previous faulting and pore pressure can easily change the principal stress orientations; thus, the model in Fig. 7 is consistent with thrust faulting in the uppermost mantle beneath the transition from the Ganga basin to the Sub-Himalaya (where the Udaypur earthquake occurred). The earthquake at a depth of 84 km and arc-perpendicular distance of around −120 km in Fig. 1 has a strike-slip mechanism with a near arc-perpendicular *P*-axis (de la Torre et al., 2007). It occurs at a location where high differential stresses are predicted in the upper mantle: In the model from Fig. 5b, the highest differential stresses take place at a depth of around 70 km, whereas in the model from Fig. 7 the greatest differential stress occurs at a depth of around 90 km. Model Suite 1 predicts a maximum in proximity to failure in the upper mantle at depths within the Indian Plate above 80 km, in contrast with results from Model Suite 2, which predict a maximum in proximity to failure at depths below 80 km within the Indian Plate. Moment tensor inversions for this earthquake using different velocity models (de la Torre et al., 2007) suggest a minimum possible depth of 75 km. Even though the predicted stress orientations at the location of the earthquake suggest thrust faulting, the difference between the vertical and the out-of-plane stresses is about 100 MPa, so the same argument used above for a possible switch between orientations consistent with thrust-faulting and strike-slip like orientations is valid for this case.

Models in Figs. 5b and 7 indicate that high differential stresses are taken up in the lithospheric mantle. These high differential stresses suggest that the response of the uppermost mantle of the Indian Plate to loading is predominantly elastic, and the viscous relaxation takes

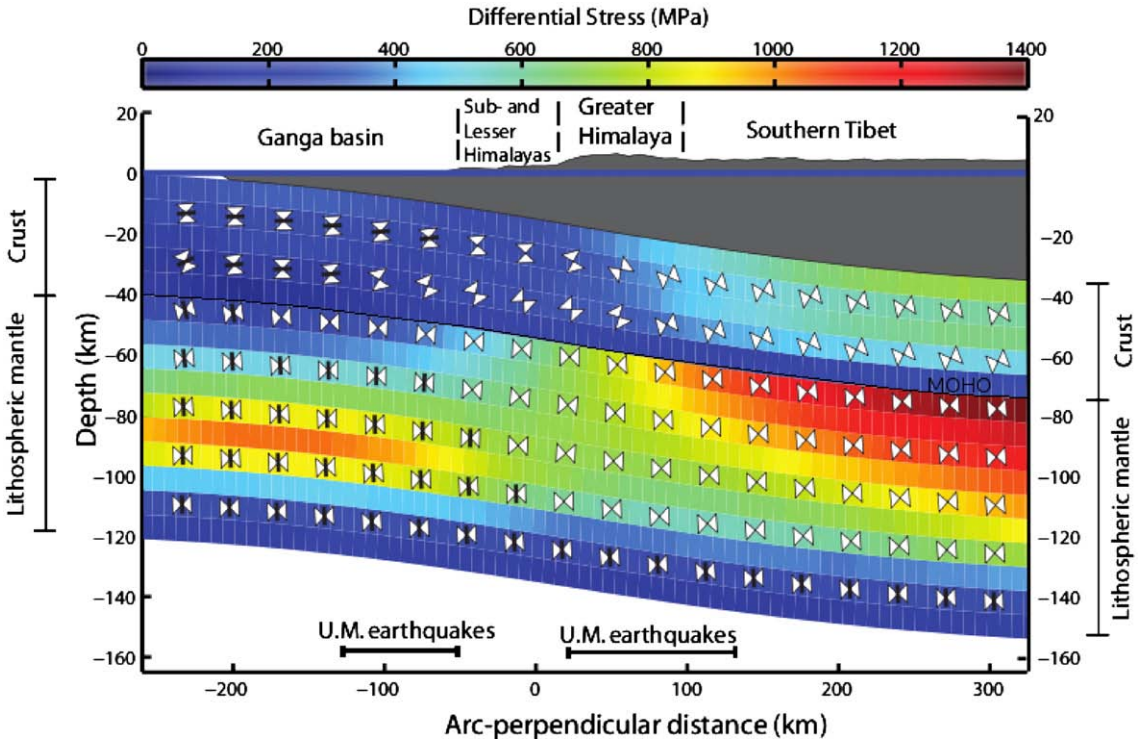

Fig. 7. Flexural profile and stress field along a Himalayan arc-perpendicular cross-section across the study region for the case of a viscoelastic crust (Model Suite 2). Effective viscosities are calculated using a power law relationship. Horizontal compression of this model corresponds to a northward displacement of the southern end of the grid of 17 km. The horizontal bars at the bottom of the models (labeled as 'U.M. earthquakes') represent the location of clusters of earthquakes at near-Moho depths. See Fig. 3 for symbol conventions.

place primarily in its lowermost part (the lowest 20 km or so of the lithospheric mantle). Regardless of the assumed kind of rheology, the models of the Indian Plate under the action of the weight of the mountain and the thrust sheets combined with horizontal compression, show differential stresses greater than 800 MPa in the upper mantle. When the crust is assumed to be elastic, the crustal portion of

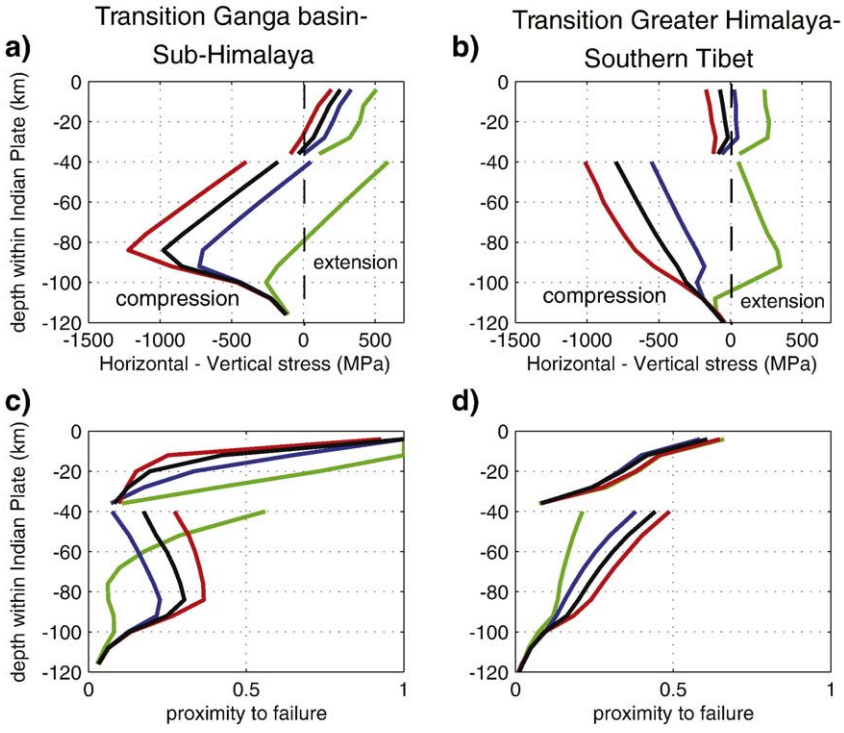

Fig. 8. Cross-sections of stress differences at the average locations of clusters with upper mantle earthquakes for different amounts of horizontal compression. Results from Model Suite 2 are shown here. Blue, black and red curves represent displacements of the southern end of the grid of 12, 17, and 22 km respectively. Since in most cases the response of the lower crust to loading is not elastic, we did not extrapolate the curves to the Moho and did not connect the crustal and mantle portions of the curves. a) Stress differences at the transition Ganga Basin–Sub-Himalaya, b) stress differences at the transition Greater Himalaya–Southern Tibet, c) proximity to failure at the transition Ganga Basin–Sub-Himalaya, d) proximity to failure at the transition Greater Himalaya–Southern Tibet.

the lithosphere takes up a significant portion of the load (Fig. 5b, Southern Tibet), but the uppermost mantle still responds elastically and high differential stresses occur there.

Plots of proximity to failure (Figs. 6c, d, 8c and d) indicate that, except for the upper crust, the lithospheric materials in the Indian Plate at the Himalayan collision zone are far from failure. In the uppermost mantle, values of proximity to failure are below 0.6 in all cases. In particular, for the profile at the location of the earthquake cluster beneath the Ganga basin and the Sub-Himalaya and a displacement of the far south boundary of 22 km (black curve from Fig. 6c and red curve from Fig. 8c), there is a significant difference between proximity to failure in the lowermost crust and in the uppermost mantle, with very low values in the lowermost crust (about 0.1). However, a decrease in the stiffness contrast between the lower crust and the upper mantle could reduce this difference in proximity to failure, and would help us better explain the occurrence of brittle failure at both sides of the Moho at this location. Thus, lateral variations in the elastic parameters, local inhomogeneities in the structure of the lower crust and other factors discussed below, should be playing a role in the yielding of materials at around Moho depths.

The proximity to failure in the uppermost mantle beneath southernmost Tibet, just north of the Greater Himalaya, is below 0.5, and is greater than immediately above it, in the lowermost crust. Therefore, given these relatively low values, there should be a mechanism that changes either the magnitude of the principal stresses or the failure envelope, so that brittle failure eventually occurs. The presence of aqueous fluids in the upper mantle can cause an increase in the pore pressure, thereby modifying the failure envelope; the principal stresses would decrease, so that faulting becomes more likely. In this region of the upper mantle, a pore pressure with a magnitude of 50 to 80% of the lithostatic pressure would be needed to cause failure of these materials. The existence, origin, spatial extent and role in the collision dynamics of such fluids are a matter of debate, but they can certainly be a determining factor in the occurrence of subcrustal earthquakes beneath southern Tibet. A possible source for aqueous fluids in the underthrusting Indian plate is the release of water in metamorphic reactions. There are several pieces of evidence for metamorphic transformations at near-Moho depths beneath southern Tibet (and probably the Greater Himalaya), most likely due to an increase in temperature and pressure of materials in the lower crust of the underthrusting Indian Plate that puts the rocks in the eclogite stability field (Monsalve et al., 2008). Peacock (1993) shows that, for a basaltic bulk composition, and for a great variety of *P*–*T* paths, the formation of eclogite is accompanied by dehydration.

Bjørnerud et al. (2002) and Jackson et al. (2004) discuss the formation of eclogite from dry granulite in the lower crust of continental collisional belts. This represents one of the few *P*–*T* paths to the eclogite stability field that is not associated with dehydration. These authors state that for this reaction to occur, an increase in the rock water content is necessary. Thus, at some point, the water source should have been different from the granulite–eclogite reaction. One alternative possibility as a source of water, other than metamorphic reactions within the Indian Plate, is the generation of aqueous fluids in the upper mantle, from metamorphic reactions that occurred within remnants of continental and oceanic Greater Indian lithosphere that detached from the presently underthrusting plate and sank into the mantle. Travel times of P-waves indicate the existence of high velocity anomalies in the upper mantle, which can be explained by these fragments of ancient Greater Indian Lithosphere (Zhou et al., 1996; Van der Voo et al., 1999).

Jackson et al. (2004) argue that rock fracturing facilitated water circulation so that the metamorphic reaction could occur. In this kind of reasoning, there is no way to know whether the water came first or the faulting did, but in any case, and whatever the water source is, the near-Moho earthquakes beneath the transition from the Greater Himalaya to south Tibet could be related to the failure of an eclogitic body, as the local earthquake tomography suggests (Monsalve et al., 2008), and the presence of aqueous fluids is likely playing a role in both the metamorphic transformations and the faulting.

5. Conclusions

The objective of the finite element modeling of the Indian Plate at the Himalayan collision was to evaluate the role of the upper mantle in the support of the loads, and the consistency of the stress orientations predicted by focal mechanisms of earthquakes below the Moho in this region. Results from the different model suites indicate that earthquakes in the upper mantle beneath the Himalayan collision are consistent with loading of a viscoelastic plate, where the main external forces acting upon it are the weight of the mountains and thrust sheets, and a horizontal force associated with the plate convergence: the orientations of focal mechanisms are reproduced by the model and high differential stresses occur in the lithospheric upper mantle, whose response to loading is predominantly elastic.

Horizontal compression of the Indian lithosphere is required in order to account for the variation of focal mechanisms with depth beneath the Ganga basin and the Himalayan foreland. The use of this in-plane force is warranted by the existence of dragging forces from the mantle and shear forces from the load acting upon the underthrusting lithosphere. We found that in this region there is no evidence of earthquakes showing normal faulting in the upper mantle, but our models suggest that this is not a necessary condition for the upper mantle to have significant participation in the support of the loads (the upper mantle is strong). Results from Model Suite 2 (Figs. 7, 8a, and b), where a viscoelatic crust is assumed, give the best match to the observations; models with an elastic crust and horizontal compression (Model Suite 1, Figs. 5b, 6a, and b) indicate that the lower crust is not required to be weak in order for the lithospheric upper mantle to respond elastically to loading and to bear a significant fraction of the stresses.

Even though the lithospheric bending can explain the high background stresses in some regions of the uppermost mantle, simple Mohr–Coulomb theory by itself does not explain the observed pattern of failure. Additional factors should play a role in bringing those materials to failure: lateral variations in elastic properties, local inhomogeneities, effects of previous faulting and high pore pressures caused by aqueous fluids released in metamorphic reactions in the deep crust or the upper mantle, are likely candidates.

Acknowledgements

We thank Sun-Lin Chun, the Managing Guest Editor of this volume, and Andrés Villavicencio, the Journal Manager of Tectonophysics. We also wish to thank an anonymous reviewer, whose comments and suggestions greatly contributed to the improvement of the manuscript. This research was funded by the National Science Foundation (NSF) and the Lunar and Planetary Institute (LPI) contribution # 1462.

References

Bilham, R., 2004. Earthquakes in India and the Himalaya: tectonics, geodesy and history. Ann. Geophys. 47 (2), 839–858.

Bilham, R., Gaur, V., Molnar, P., 2001. Himalayan seismic hazard. Science 293, 1442–1444.

Bilham, R., Bendick, R., Wallace, K., 2003. Flexure of the Indian Plate and intraplate earthquakes. Proc. Indian Acad. Sci. (Earth Planet Sci.) 112, 1–14.

Bjørnerud, M., Austrheim, H., Lund, M., 2002. Processes leading to eclogitization (densification) of subducted and tectonically buried crust. J. Geophys. Res. 107. doi:10.1029/2001JB000527.

Burov, E., Diament, M., 1995. The effective elastic thickness (Te) of continental lithosphere: what does it really mean? J. Geophys. Res. 100, 3905–3927.

Burov, E., Watts, A., 2006. The long-term strength of continental lithosphere: "jelly sandwich" or "creme brulee". GSA Today 16, 4–10.

Cattin, R., Avouac, J., 2000. Modeling mountain building and the seismic cycle in the Himalaya of Nepal. J. Geophys. Res. 105, 13,389–13,407.

Chen, W., Kao, H., 1996. Seismotectonics of Asia: some recent progress. In: Yin, A., Harrison, M. (Eds.), The Tectonic Evolution of Asia, pp. 37–62.
Chen, W., Molnar, P., 1983. Focal depths of intracontinental and intraplate earthquakes and their implications for the thermal and mechanical properties of the lithosphere. J. Geophys. Res. 88, 4183–4214.
Chen, W., Yang, Z., 2004. Earthquakes beneath the Himalayas and Tibet: evidence for strong lithospheric mantle. Science 304, 1949–1952.
Chen, W., Nabelek, J., Fitch, T., Molnar, P., 1981. An intermediate depth earthquake beneath Tibet: source characteristics of the event of September 14, 1976. J. Geophys. Res. 86, 2863–2876.
de la Torre, T.L., Monsalve, G., Sheehan, A., Sapkota, S., Wu, F., 2007. Earthquake processes of the Himalayan collision zone in Eastern Nepal and the Southern Tibetan Plateau. Geophys. J. Int. 171, 718–738. doi:10.1111/j.1365-246X.2007.03537.x.
Engdahl, E., der Hilst, R.V., Buland, R., 1998. Global teleseismic earthquake relocation with improved travel times and procedures for depth determination. Bull. Seismol. Soc. Am. 88, 722–743.
Feldl, N., Bilham, R., 2006. Great Himalayan earthquakes and the Tibetan plateau. Nature 444, 165–170.
Goetze, C., 1978. The mechanisms of creep in olivine. Phil. Trans. R. Soc. Lond. 288, 99–119.
Goetze, C., Evans, B., 1979. Stress and temperature in the bending lithosphere as constrained by experimental rock mechanics. Geophys. J. R. astron. Soc. 59, 463–478.
Henry, P., LePichon, X., Goffe, B., 1997. Kinematic, thermal and petrological model of the Himalayas: constraints related to metamorphism within the underthrust Indian crust and topographic elevation. Tectonophysics 273, 57–76.
Hetényi, G., Cattin, R., Vergne, J., Nabelek, J., 2006. The effective elastic thickness of the India Plate from receiver function imaging, gravity anomalies and thermomechanical modelling. Geophys. J. Int. 167, 1106–1118.
Jackson, J., 2002. Strength of the continental lithosphere: time to abandon the jelly sandwich? GSA Today 12, 4–10.
Jackson, J., Austrheim, H., Mckenzie, D., Priestley, K., 2004. Metastability, mechanical strength, and the support of mountain belts. Geology 32, 625–628.
Jordan, T., Watts, A., 2005. Gravity anomalies, flexure and the elastic thickness structure of the India–Eurasia collisional system. Earth Planet. Sci. Lett. 236, 732–750.
Lomax, A. (2004), Probabilistic, non-linear, global-search earthquake location in 3D media, Anthony Lomax Scientific Software, Mouans–Sartoux, France.
Maggi, A., Jackson, J., McKenzie, D., Priestley, K., 2000a. Earthquake focal depths, effective elastic thickness and the strength of the continental lithosphere. Geology 28, 495–498.
Maggi, A., Jackson, J., Priestley, K., Baker, C., 2000b. A reassessment of focal depth distributions in Southern Iran, the Tien Shan and Northern India: do earthquakes really occur in the continental mantle? Geophys. J. Int. 143, 629–661.
McGovern, P., 2007. Flexural stresses beneath Hawaii: implications for the October 15, 2006, earthquakes and magma ascent. Geophys. Res. Lett. 34. doi:10.1029/2007GL031305.
McGovern, P., Solomon, S., 1993. State of stress, faulting, and eruption characteristics of large volcanoes on Mars. J. Geophys. Res. 98, 23,553–23,579.
McGovern, P., Solomon, S., 1998. Growth of large volcanoes on Venus: mechanical models and implications for structural evolution. J. Geophys. Res. 103, 11,071–11,101.
Melosh, H., Raefsky, A., 1980. The dynamical origin of subduction zone topography. Geophys. j. R. Astron. Soc. 60, 333–354.
Melosh, H., Raefsky, A., 1983. Growth of large volcanoes on Venus: mechanical models and implications for structural evolution. J. Geophys. Res. 88, 515–526.
Mitra, S., Priestley, K., Bhattacharyya, A., Gaur, V., 2005. Crustal structure and earthquake focal depths beneath northeastern India and southern Tibet. Geophys. J. Int. 160, 227–248. doi:10.1111/j.1365-246X.2004.02470.x.
Mitrovica, J., Forte, A., 2004. A new inference of mantle viscosity based upon joint inversion of convection and glacial isostatic adjustment data. Earth Planet. Sci. Lett. 225, 177–189.
Molnar, P., Chen, W., 1983. Focal depths and fault plane solutions of earthquakes under the Tibetan Plateau. J. Geophys. Res. 88, 1180–1196.
Molnar, P., Jones, C., 2004. A test of laboratory based rheological parameters of olivine from an analysis of late Cenozoic convective removal of mantle lithosphere beneath the Sierra Nevada, California, USA. Geophys. J. Int. 156, 555–564. doi:10.1111/j.1365-246X.2004.02138.x.
Molnar, P., Tapponnier, P., 1978. Active tectonics of Tibet. J. Geophys. Res. 83, 5361–5375.
Monsalve, G., Sheehan, A., Schulte-Pelkum, V., Rajaure, S., Pandey, M., Wu, F., 2006. Seismicity and 1-D velocity structure of the Himalayan collision zone: earthquakes in the crust and upper mantle. J. Geophys. Res. 111 (B10301). doi:10.1029/2005JB004062.
Monsalve, G., Sheehan, A.F., Rowe, C., Rajaure, S., 2008. Seismic structure of the crust and the upper mantle beneath the Himalayas: evidence for eclogitization of lower crustal rocks in the Indian Plate. J. Geophys. Res. 113 (B08315). doi:10.1029/2007JB005424.
Mouthereau, F., Petit, C., 2003. Rheology and strength of the Eurasian continental lithosphere in the foreland of the Taiwan collision belt: constraints from seismicity, flexure, and structural styles. J. Geophys. Res. 108. doi:10.1029/2002JB002098.
Mueller, S., Phillips, R.J., 1995. On the reliability of lithospheric constraints derived from models of outer-rise flexure. Geophys. J. Int. 123, 887–902.
Pandey, M., Tandukar, R., Avouac, J., Lavé, J., Massot, J., 1995. Interseismic strain accumulation on the Himalayan crustal ramp (Nepal). Geophys. Res. Lett. 22, 751–754.
Paulson, A., Zhong, S., Wahr, J., 2007. Inference of mantle viscosity from GRACE and relative sea level data. Geophys. J. Int. 171, 497–508. doi:10.1111/j.1365-246X.2007.03556.x.
Peacock, S., 1993. The importance of blueschist–eclogite dehydration reactions in subducting oceanic crust. Geol. Soc. Am. Bull. 105, 684–694.
Priestley, K., Jackson, J., McKenzie, D., 2008. Lithospheric structure and deep earthquakes beneath India, the Himalaya and southern Tibet. Geophys. J. Int. 172, 345–362. doi:10.1111/j.1365-246X.2007.03636.x.
Pritchard, M., Rubin, A., Wolfe, C., 2007. Do flexural stresses explain the mantle fault zone beneath Kilauea volcano. Geophys. J. Int. 168, 419–430.
Schulte-Pelkum, V., Monsalve, G., Sheehan, A., Pandey, M., Sapkota, S., Bilham, R., 2005. Imaging the Indian subcontinent beneath the Himalaya. Nature 435, 1222–1225.
Steinberger, B., Calderwood, A., 2006. Models of large-scale viscous flow in the Earth's mantle with constraints from mineral physics and surface observations. Geophys. J. Int. 167, 1461–1481.
Thurber, C., Gripp, A., 1988. Flexure and seismicity beneath the south flank of Kilauea volcano and tectonic implications. J. Geophys. Res. 93, 4271–4278.
Van der Voo, R., Spakman, W., Bijwaard, H., 1999. Tethyan subducted slabs under India. Earth Planet. Sci. Lett. 171, 7–20.
Watts, A., 2001. Isostasy and flexure of the lithosphere. Cambridge University Press.
Watts, A., Burov, E., 2003. Lithospheric strength and its relationship to the elastic and seismogenic layer thickness. Earth Planet. Sci. Lett. 213, 113–131.
Wolfe, C., Okubo, P., Shearer, P., 2003. Mantle fault zone beneath Kilauea volcano, Hawaii. Science 300, 478–480.
Zhao, W., Nelson, K., Project INDEPTH Team, 1993. Deep seismic reflection evidence for continental underthrusting beneath southern Tibet. Nature 366, 557–559.
Zhou, R., Grand, S., Tajima, F., Ding, X., 1996. High velocity zone beneath the southern Tibetan plateau from P-wave differential travel-time data. Geophys. Res. Lett. 23, 25–28.
Zhu, L., Helmberger, D., 1996. Intermediate depth earthquakes beneath the India–Tibet collision zone. Geophys. Res. Lett. 23, 435–438.